View metadata, citation and similar papers at core.ac.uk
brought to you by CORE
provided by Elsevier - Publisher Connector

Equivalent Aqueous Phase Modulation of Domain Segregation in Myelin Monolayers and Bilayer Vesicles

Rafael G. Oliveira,[†‡*] Emanuel Schneck,[‡§] Sergio S. Funari,[¶] Motomu Tanaka,[‡§] and Bruno Maggio[†]
[†]Centro de Investigaciones en Química Biológica de Córdoba, Universidad Nacional de Córdoba, Ciudad Universitaria, Córdoba, Argentina; [‡]Department of Physics, Technical University of Munich, Garching, Germany; [§]Biophysical Chemistry, Institute of Physical Chemistry, and BIOQUANT, University of Heidelberg, Heidelberg, Germany; and [¶]HASYLAB at Deutsches Elektronen Synchrotron, Hamburg, Germany

ABSTRACT Purified myelin can be spread as monomolecular films at the air/aqueous interface. These films were visualized by fluorescence and Brewster angle microscopy, showing phase coexistence at low and medium surface pressures (<20–30 mN/m). Beyond this threshold, the film becomes homogeneous or not, depending on the aqueous subphase composition. Pure water as well as sucrose, glycerol, dimethylsulfoxide, and dimethylformamide solutions (20% in water) produced monolayers that become homogeneous at high surface pressures; on the other hand, the presence of salts (NaCl, $CaCl_2$) in Ringer's and physiological solution leads to phase domain microheterogeneity over the whole compression isotherm. These results show that surface heterogeneity is favored by the ionic milieu. The modulation of the phase-mixing behavior in monolayers is paralleled by the behavior of multilamellar vesicles as determined by small-angle and wide-angle x-ray scattering. The correspondence of the behavior of monolayers and multilayers is achieved only at high surface pressures near the equilibrium adsorption surface pressure; at lower surface pressures, the correspondence breaks down. The equilibrium surface tension on all subphases corresponds to that of the air/alkane interface (27 mN/m), independently on the surface tension of the clean subphase.

INTRODUCTION

Myelin constitutes the membrane material surrounding axons. It has a low protein content (25% w/w), with a few major proteins such as the Folch's proteolipid (50%), myelin basic protein (MBP) (30%), and 2′,3′-cyclic nucleotide 3′-phosphodiesterase (10%). The lipids are mainly saturated, with mole fractions of 0.4 for phospholipids, 0.4 for cholesterol, and 0.2 for glycosphingolipids. Owing to its periodic multilayer structure, myelin is among the natural biomembranes that have been intensively studied by diffraction techniques, even under in vivo conditions. The existence of lateral structural heterogeneity in native bulk central nervous system (CNS) myelin is controversial; on the one hand, classical x-ray scattering work tends to show bulk myelin as homogeneous, with a single lamellar spacing (1). On the other hand, certain specializations occur at the borders of the myelin sheet and in some radial and longitudinal boundaries, but the bulk of myelin was generally accepted to be rather structurally homogeneous, unless exposed to some physico-chemical treatments. Diffraction studies as well as electron microscopy showed that membrane-membrane interactions (spacing and periodicity) are sensitive to changes in osmotic pressure, ionic strength ((2) and references therein), divalent cations, anesthetics (3), dehydration (4), or freezing (5) that can lead to phase separation.

Over the last decade, we have prepared and comprehensively characterized myelin monolayers at the air-aqueous interface in terms of their stability, packing behavior, and compositional phases (6). The overall lipid and protein composition of myelin was shown to be maintained in these monolayers (7). Phase coexistence in the films was observed with fluorescent probes (8) and Brewster angle microscopy, as well as by immuno- or ligand-labeling after film transfer onto solid support (9,10). Labeling of transferred monolayer onto solid supports showed that the more-condensed phase, enriched in cholesterol and cerebroside, was depleted of proteins while another liquid-expanded (LE) phase captured the major proteins of myelin and some compressible lipids (9). In contrast to other approaches (multilayers, myelin in vivo, etc.), the monolayer technique allows a precise control of parameters such as lateral molecular packing, surface pressure, and electrostatic surface potential of a film on which direct microscopic observations of the surface pattern can be simultaneously made (8,10–12). This work adds new observations on the effects of the subphase conditions on the surface microheterogeneity of myelin monolayers.

An intermediate system between myelin in vivo and its monolayer is represented by the isolated myelin in the form of multi- or oligolamellar membranes, a material from which the monolayer can be prepared (7). Knowledge of the vesicle structure is relevant (13) because they constitute the starting material for many biochemical and topological studies. It has been established that the isolated CNS myelin membrane structure does not differ significantly from that of nerve myelin in vivo (14). Thus, understanding structural features of isolated myelin membranes in relation to its monolayer behavior provides useful comparisons to establish possible correlations to what is known for nerve

Submitted April 15, 2010, and accepted for publication June 17, 2010.

*Correspondence: oliveira@mail.fcq.unc.edu.ar

Editor: Huey W. Huang.

© 2010 by the Biophysical Society

0006-3495/10/09/1500/10 $2.00

doi: 10.1016/j.bpj.2010.06.053

myelin (1). Correlations of the behavior of monolayers and bilayers have been established for simple systems such as pure phospholipids (15,16) pulmonary surfactant (17), or lipid extracts (18). Here we attempt to expand these correlations into a system that has the full complexity of a natural membrane, and includes all of its proteins.

The objective of this work is twofold. First, we studied the influence of environmental conditions (surface pressure, lateral molecular packing, and aqueous content of hydrophilic solutes) on the phase separation in myelin monolayers. Second, we studied the extent to which isolated myelin membranes in bulk are influenced by the same conditions.

Epifluorescence and Brewster angle microscopy were coupled to a Langmuir trough on which we formed myelin monolayers. SAXS/WAXS were the techniques used to characterize the isolated myelin membrane structure.

MATERIALS AND METHODS

Chemicals

The fluorescence-labeled lipid *n*-(lissamine rhodamine B sulfonyl) diacyl phosphatidylethanolamine was purchased from Avanti Polar Lipids (Alabaster, AL). Its acyl chains are 55% unsaturated, so that the molecules get enriched in the LE phase while being excluded from more condensed cholesterol-enriched phases. Highly purified myelin was prepared from bovine spinal cord according to Haley et al. (19). Briefly, the purification protocol consists of several osmotic shocks and direct, as well as inverse, sucrose gradient centrifugations to discard gray matter constituents according to density. After three rinses in water, the myelin membranes were lyophilized and stored at −20 or −70°C. Chemicals were of analytical degree and purchased from Merck (Darmstadt, Germany).

Monolayers at the air/water interface

Lyophilized myelin was hydrated in water and homogenized by extrusion (five times through a 26G needle fitted to a syringe). Monolayers were formed by spreading a suspension (~0.2–0.5 protein mg/mL) of myelin membranes onto the surface of the aqueous phase. To improve the spreading yield, 5% ethanol was added occasionally to the membrane suspension. This addition did not alter the compression isotherm or the patterns observed under the microscope. For fluorescence microscopy observation, the monolayers were doped with 0.5–1 mol % of *n*-(lissamine rhodamine B sulfonyl) diacyl phosphatidylethanolamine. The subphases (room temperature 23 ± 2°C) were:

Phase A, bidistilled water;
Phase B, 20% glycerol;
Phase C, 20% sucrose;
Phase D, 20% Dimethylsulfoxide (DMSO);
Phase E, 20% Dimethylformamide (DMF);
Phase F, NaCl 100–145 mM;
Phase G, Ringer's solution (145 mM NaCl, 6 mM KCl, 2 mM $CaCl_2$, 2 mM $MgCl_2$, pH 7.4 with 1.5 mM $NaHCO_3$/NaH_2PO_4 buffer);
Phase H, 20 or 33 mM $CaCl_2$ in Ringer's;
Phase I, 20% DMSO in Ringer's and
Phase J, 20% DMF in Ringer's.

All the subphases were checked for absence of surfactants as previously described (20).

The surface pressure reached in the initial spreading was <0.3 mN/m. The films were compressed at different rates; typically the isotherm took 10–60 min. Five-to-fifteen minutes of equilibration were allowed after each change of surface pressure before image capturing, and in the special case of pattern homogenization, up to 2 h.

The observations were carried out under isometric compression of the films, at room temperature (9), using a Minitrough II (KSV, Helsinski, Finland) or a Microtrough (Kibron, Espoo, Finland) mounted on the microscope stage. An open-end Teflon mask with a lateral vertical slit, extending through the film into the subphase, was occasionally used to restrict the flow of the monolayer in the field being observed. Axioplan or Axiovert (Carl Zeiss, Oberkochen, Germany) epifluorescence microscopes were used, equipped with a mercury lamp HBO 50 and objectives of 10 and 20×. Exposure times were ~100 ms. The images were recorded by a charge-coupled device video camera, an Axiocam HRC, commanded through Axiovision software (Carl Zeiss). Occasionally Brewster angle microscopy (BAM) (21,22) was used. Here, essentially the same procedure as in epifluorescence microscopy was followed, but without using fluorescent probes. A MiniBAM plus microscope or EP3 imaging ellipsometer (in BAM setup) were used (both from Nanofilm Technologies, Gottingen, Germany).

Equilibrium surface pressure

Equilibrium surface pressure (ESP) is the surface pressure at which the interfacial adsorbed Gibb's film is in equilibrium with the membrane material in the subphase. We performed this measurement to determine the packing state in the spread Langmuir monolayer that most closely resembles the above-mentioned equilibrium condition. This was actually measured by sprinkling a small amount of powdered lyophilized myelin over the aqueous interface and allowing equilibration. The same value is attained by injecting myelin vesicles in the subphase or by depositing an excess of solvent-solubilized myelin. To ascertain whether the surface-pressure reached corresponded to the ESP, the film was slightly overcompressed or decompressed, then allowed to time-relax (23). By doing this, the same value of the ESP was reached (24).

Small-angle x-ray scattering of myelin membrane suspensions

Small-angle x-ray scattering (SAXS) was simultaneously performed with wide-angle x-ray scattering (WAXS). SAXS was used to determine the regular spacing periodicity between bilayers, and WAXS to detect possible variations of acyl-chain ordering. For sample preparation, 2–3 mg of lyophilized myelin were introduced in quartz capillaries of 1-mm diameter, and 10 μL of aqueous solutions added. The capillaries were flame-sealed and subsequently centrifuged. Thawing and cooling cycles were performed (4–40°C) and stored at 4°C until measurements at room temperature. Measurements were performed at the beamline A2 at HASYLAB (Deutsches Elektronen Synchrotron, Hamburg, Germany), at a fixed wavelength of 1.5 Å. A linear position-sensitive gas-filled detector was used, and in some cases, a two-dimensional detector (MAR CCD 165; Rayonix, Evanston, IL). The typical sample-detector distance was 1.80 m. Additional measurements were performed at the DO2A:SAXS2 (Laboratório Nacional de Luz Síncrotron, Campinas, Brazil). In this case, lyophilized myelin was suspended at 25 mg/mL, warmed up to 45°C to ensure hydration, and filled into the sample holder between two mica plates. Here, 1.488 Å radiation was used and the sample detector distance was 1 m. For radial integration of the Debye-Scherrer rings on the two-dimensional detector, we employed the free software Fit2D V12.077 from Andy Hammersley at the European Synchrotron Radiation Facility (Grenoble, France).

RESULTS

Compression isotherms and ESP of monolayers

Globally, all the compression isotherms (data not shown) are quite similar to the one previously published (7). On water,

the monolayer collapses in the range 44–47.5 mN/m, unless 20% DMSO or DMF are added to the solution, where the isotherms show lower collapse pressures (36 and 27 ± 1 mN/m, respectively). By contrast, on a high salt (5 M NaCl) subphase, the myelin film collapses at higher surface pressure (53 mN/m). Generally, the films showed compressibilities typical of the LE phase.

Within the experimental error (±1 mN/m), the equilibrium surface pressure (ESP) is identical to the collapse pressure for all subphases. Moreover, the surface tensions of the monolayers (plotted in Fig. 1) level off to the same final surface tension (26–28 mN/m) after reaching equilibrium, although the blank subphases possess different initial surface tensions. Table 1 summarizes the characteristics of all compression isotherms.

Microscopy of monolayers

Typical pictures of monolayers on various salt-free subphases (subphases *A–E*) are presented in Fig. 2 at three selected surface pressures: low (1–3 mN/m, starting isotherm), medium (10–20 mN/m), and high (20–40 mN/m, slightly below collapse). Fig. 3 shows the pattern observed on ionic solutions (subphases *F–J*). As can be seen from the comparison of Figs. 2 and 3, the results can be classified into two behaviorally different groups, as follows.

Behavior 1 (I_{film})

At low surface pressures, isolated dark cholesterol-enriched liquid domains are found within a continuous LE phase. The monolayer assumes a homogeneous phase at higher pressures (15–35 mN/m) and shows no percolation transition (Fig. 2).

Behavior 2 (II_{film})

At low surface pressure, isolated liquid-expanded domains are found within a continuous dark phase. A percolation transition takes place at 10–20 mN/m, but the phase coexistence remains up to the monolayer collapse pressure (Fig. 3). The time needed for the formation of

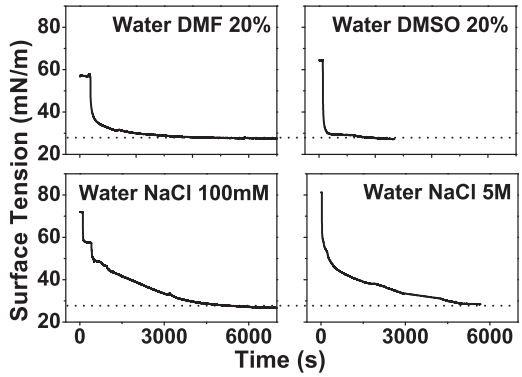

FIGURE 1 Myelin monolayer equilibrium surface tension on different subphases. Typical surface tension curves over time are shown on different subphases. Note the convergence to the same equilibrium value, despite the original surface tension of the clean subphase before monolayer spreading. (*Horizontal dotted lines*) References at 27 mN/m.

TABLE 1 Critical parameters for collapse and surface phase homogenization of myelin monolayers as a function of the subphase

Subphase	γ [mN/m]	π_c [mN/m]	γ_c [mN/m]	π_t [mN/m]	γ_t [mN/m]
Water	72	45	27	35	37
Water glycerol 20%	72	46	26	20	52
Water sucrose 20%	72	46	26	20	52
Water DMSO 20%	64	36	28	25	39
Water DMF 20%	56	28	28	20	36
Water NaCl 100 mM	73	46	27	—	—
Ringer's	73	47	26	—	—
Tris-Ca 20 mM	73	47	26	—	—
Ringer's DMSO 20%	63	36	27	—	—
Ringer's DMF 20%	56	30	26	—	—
NaCl 5 M	81	53	28	—	—

The value γ is the surface tension of the pure subphase (before monolayer spreading), π_c is the collapse pressure of the monolayer, γ_c is the collapse surface tension, which is constant over all the conditions (taking into account the experimental error ±1 mN/m); and π_t and γ_t are the surface pressure and surface tension, respectively, for attaining surface phase homogeneity under microscopic observation. The pressure and tension values for homogenization are approximate, with an error of ~±5 mN/m. Symbol key: —, not attainable.

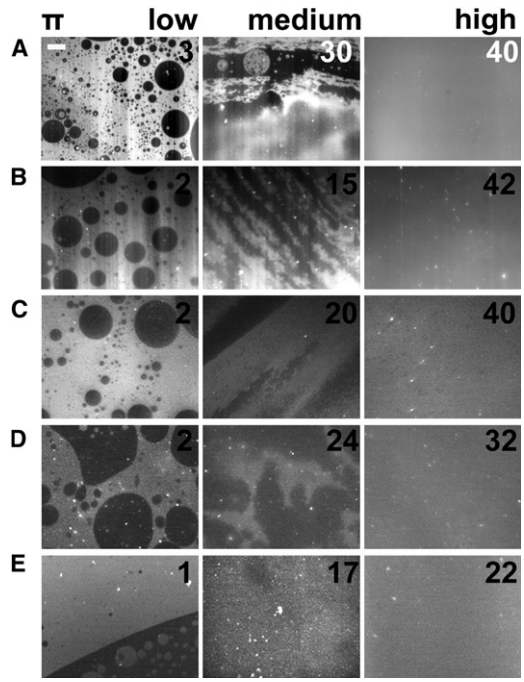

FIGURE 2 Pattern I_{film} of myelin monolayers at the air/aqueous interface (non-ionic subphase) under three different lateral packing conditions (the numbers on the pictures indicate the surface pressures: π). The capital letters (from *A* to *E*) designate the subphase according to Materials and Methods. The patterns show fluid-to-fluid coexistence with the dark phase predominantly dispersed as round domains within the brilliant phase. Under compression, the patterns blur and become homogeneous. Under expansion, the phase coexistence reappears at approximately the same surface pressures (data not shown). The scale bar is 50 μm in length.

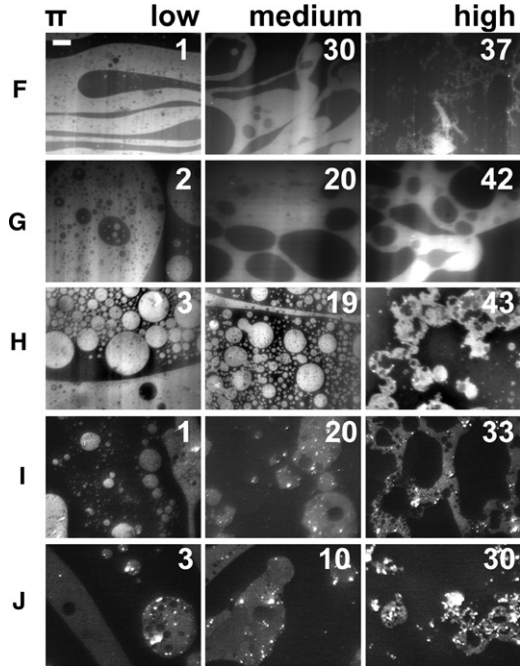

FIGURE 3 Pattern II of myelin monolayers at the air/water interface (ionic subphase) at three different lateral packing conditions (the numbers on the pictures indicate the surface pressures: π). The capital letters (from *F* to *J*) designate the subphase according to the description in the Materials and Methods. The patterns show fluid-to-fluid coexistence with the liquid-expanded phase (brilliant) predominantly dispersed within the dark phase. Under compression, the brilliant phase undergoes a percolation transition, forming fractal-like structures. The phase coexistence is present over the whole surface pressure range. The scale bar is 50 μm in length.

a homogeneous pattern in an I_{film} at high pressures is quite variable, but typically was ~1 h. The surface pressure for homogenization is also variable within ± 5 mN/m, which could be related to a variable degree of oxidation of lipids at the interface. The very first steps of myelin monolayer homogenization in a rapid compression on a DMF containing subphase can be observed in Movie S1 in the Supporting Material. II_{films} did not become homogenous even after several hours.

To verify whether the apparent homogenization in I_{films} at high pressures observed with fluorescence microscopy is not an artifact due to redistribution of the fluorescent probe, we investigated the films by Brewster angle microscopy. As illustrated in Fig. 4, on pure water, domains are observed at low surface pressures, but the film becomes homogeneous on crossing 35 mN/m, confirming the epifluorescence microscopy results.

WAXS

Lyophilized myelin was suspended in the same set of aqueous solutions that were used as monolayer subphases. In all solutions, the recorded WAXS signals exhibited a broad intensity maximum at ~$q = 1.4$ Å^{-1}, corresponding

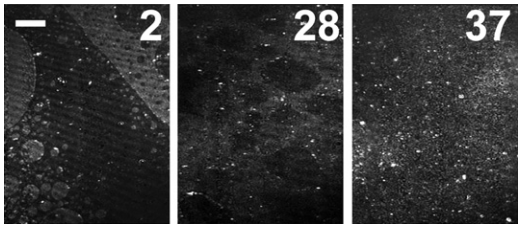

FIGURE 4 Brewster angle microscopy of myelin monolayer on pure water surface. The film is heterogeneous at low surface pressure (*first image*, 2 mN/m) with sharp domains edges; occasionally, myelin vesicles are observed as brilliant points at the lateral interfaces. At high surface pressure (~30–35 mN/m), the domain borders become diffuse and the film becomes homogeneous in 1 h above 35 mN/m, similar to the fluorescence observations. The bar is 50-μm long.

to a structure size of 4.5 Å, typical for alkanes in a liquid state (Fig. 5). Unsuspended lyophilized myelin powder (Fig. 5, *inset*) shows a major peak corresponding to alkane chains in an ordered phase with a spacing of 4.18 Å (25), and some other less intensive peaks (Fig. 5, *inset*) corresponding to unidentified, larger periodic structures (4.87, 5.09, and 5.19 Å).

SAXS

Fig. 6 shows the Debye-Scherrer rings in the SAXS setup for all the solutions presented in Figs. 2 and 3. In salt-free solutions, the radii of the rings in the diffraction patterns indicate well-ordered lamellar structures with one single periodicity each (*first column* in Fig. 6). This behavior is called I_{bulk} in the following. Fig. 7 *A* shows the radially integrated intensity spectrum (diffractogram) of myelin suspended in pure water as a function of q. The diffractograms show a weak intensity maximum at ~$q = 0.407$ nm^{-1}, corresponding to a lamellar periodicity of ~155 Å. It can be

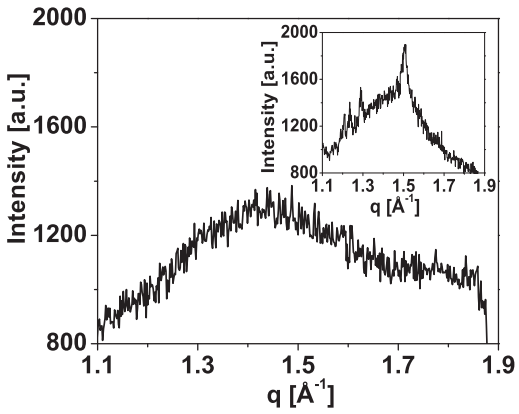

FIGURE 5 Representative WAXS data at 20°C for hydrated myelin (water glucose 20%). (*Inset*) Dehydrated powder shows crystalline-like order centered at 4.15 Å (plus other minor peaks). Hydrated samples always show the broad peak shifted to lower q values, centered at ~4.4 Å, characteristic of liquid-like acyl chains.

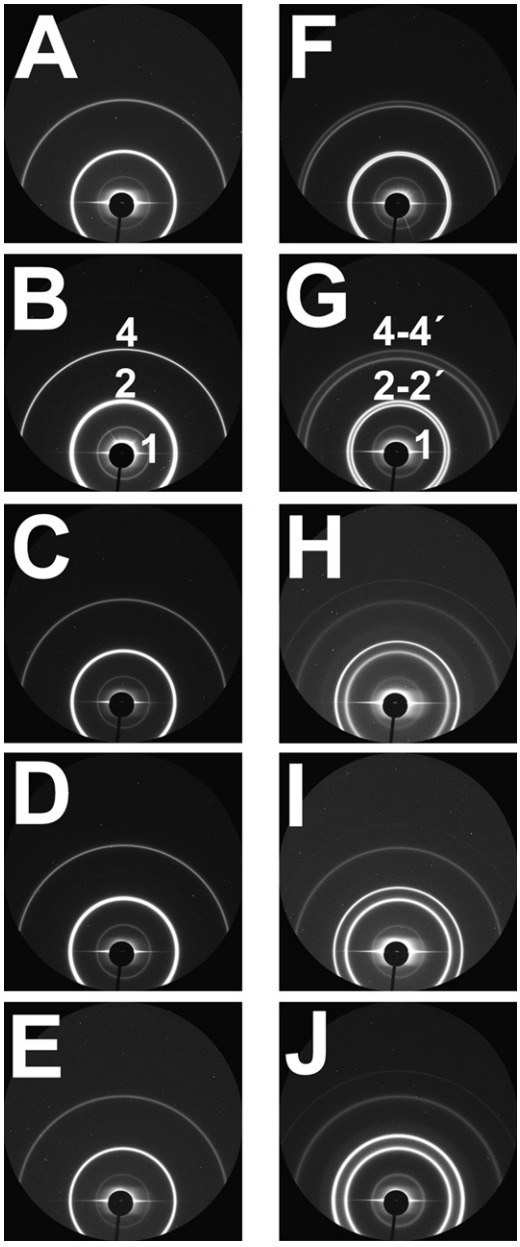

FIGURE 6 Raw SAXS data from the two-dimensional detector for myelin vesicles. The dominant signal is the one corresponding to the second-order and fourth-order harmonic (shown as 2 and 4, respectively). The samples *A–E* in the first column (see Materials and Methods) show single Bragg diffraction peaks corresponding to the normal spacing in CNS myelin (~155 Å). The second column (*F–J*) shows the splitting of the Debye-Scherrer rings (labeled as 2-2′ and 4-4′) in salt-containing media; the ring-splitting points to the existence of two phases.

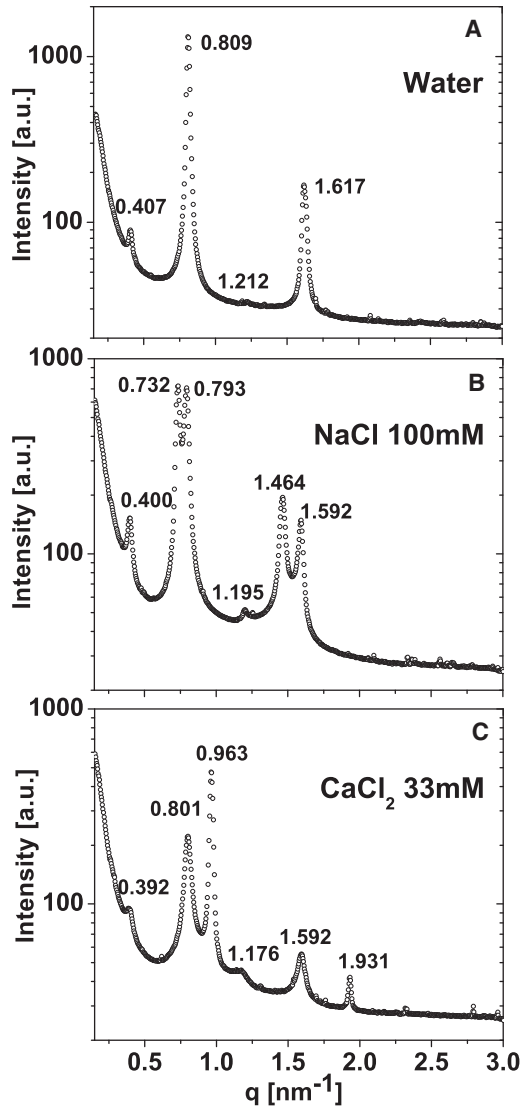

FIGURE 7 Selected SAXS data showing three conditions: (*A*) Pattern I_{bulk} for myelin vesicles in water. (*B*) Pattern $II_{bulk\text{-}e}$ for vesicles in NaCl 100 mM. (*C*) Pattern $II_{bulk\text{-}c}$ for vesicles in $CaCl_2$ 33 mM.

well explained with an asymmetric unit cell composed of two myelin membranes. This clearly indicates that the bilayer asymmetry of myelin (1) is well preserved during the sample preparation. The highest intensity peak ($q = 0.809$ nm^{-1}) corresponding to a periodicity of ~77 Å is in excellent agreement with the diffractogram of isolated and nerve CNS myelin. These observations are in good agreement with what is known from optic nerve and isolated CNS myelin in pure water (26). At moderate concentrations (<20% V/V), non-ionic solutes (sucrose, glycerol, DMSO, or DMF) have no major effect on the SAXS patterns (Fig. 6, *first column*). By contrast, the addition of NaCl or $CaCl_2$ results in a clear radial splitting of the rings (Fig. 6, *second column*), which has to be interpreted as the coexistence of membrane phases with different lamellar periodicities. The same is observed with Ringer- and Tris-buffer-based solutions (pH 7.4) of sufficiently high ionic content (Fig. 6). This behavior is called II_{bulk} in the following. This resembles the domain behavior classification in monolayers (I_{film} and II_{film}, see before). In fact, there is a full correspondence in the response of monolayers and bilayers to the different aqueous environments: Phase

coexistence in myelin monolayers and bilayers is induced by the same conditions. Thus, I_{film} in monolayers corresponds to I_{bulk} in bilayer suspensions, and pattern II_{film} corresponds to pattern II_{bulk}.

In a closer inspection, it is seen that there are two distinct types of phase coexistence in the isolated myelin. This is shown in Fig. 7 for some representative conditions (water, water-NaCl, and water-$CaCl_2$). Panel *A* presents the diffractogram of isolated myelin in pure water which exhibits a single lamellar spacing of 155 Å (no phase separation). This coincides with the spacing of 155 Å found for asymmetric native CNS myelin double bilayers (26). In Ringer (and its mixtures with glucose or glycerol) as well as in water-NaCl, two lamellar spacings are seen in the diffractograms, one close to the spacing of native myelin bilayers (79.2 Å) and another larger one (85.8 Å). In the following, this type of phase coexistence is referred to as $II_{bulk\text{-}e}$ (*e* for expanded). By contrast, the addition of Ca^{2+}, as well as DMSO and DMF to the Ringer solution, results in a different set of lamellar spacings (78.4 Å and 65.2 Å). The smaller value reveals a highly compacted structure. In the following, this type of phase coexistence is referred to as $II_{bulk\text{-}c}$ (*c* for compacted). Both kinds of phase coexistence have been previously reported for CNS myelin in nerve (1,2,27), which demonstrates that the isolated myelin preserves an environmental sensitivity analogous to the one displayed by nerve myelin.

DISCUSSION

Seminal work had been performed more than 25 years ago on myelin phase homogeneity/heterogeneity, mainly by diffraction techniques (1). Here, we compare these results with simplified, monolayer-isolated myelin, with a focus on the influence of the aqueous medium on the phase behavior of monolayers and multilamellar vesicles. Our results reveal a strong similarity between these systems, despite the obvious structural differences.

Compression isotherms and ESP

Langmuir monolayers at the air/water interface can be compressed over a wide range of molecular areas (and, inherently, surface pressures) at which the lateral film organization is quite different. This leads to the question of which situation comes closest to that in native membranes (28–30), and this is still under debate (31,32). Previously, we have shown that for the case of myelin, vesicles adsorb to the air/aqueous interface up to the collapse pressure (45–47 mN/m), at which monolayers typically coexist with multilayers (24). Because the multilayers in bulk suspension and the interfacial film are in equilibrium at this state, this would be a reasonable equivalent condition to compare the monolayer properties to those of isolated myelin membrane vesicles (29). Therefore, we used the surface micrographs obtained at high surface pressure (near collapse) for a comparison with the phase properties of the bulk suspension studied by SAXS. For DMSO and DMF 20% solutions, the collapse surface pressures are lower, but still equal to the corresponding ESP.

Constant equilibrium surface tension

We pointed out previously that myelin adsorbs spontaneously up to a surface pressure of 45–47 mN/m, independent of temperature (24). Now we extended those observations and show that this constancy is also independent of the presence of hydroxylated solutes. Additionally, we show that the introduction into the subphase of aprotic solvents (DMSO and DMF) causes lowering of the collapse pressure and of the ESP by 6 and 16 mN/m. Noticeably, the surface tension of those film-free subphases compared to pure water is also lower by 6 and 16 mN/m, respectively, and the ESP decreases by the same amount as the surface tension of the corresponding clean subphase.

Because $\pi = \gamma_{subphase} - \gamma_{film}$, the surface tension at collapse and at the equilibrium adsorption in Gibb's films (26–28 mN/m) is independent of the subphase composition. Previously, the constancy of ESP (24) was due to the constant initial surface tension of the clean subphases. Our present use of subphases with different initial surface tensions reveals that, at equilibrium, it is not the surface pressure (commonly used in analysis in the literature) that is constant; it is the surface tension that is constant. This is why we show the data in Fig. 1 in terms of surface tension. The commonly employed salt solutions (at ~0–0.1 M) do not modify appreciably the surface tension compared to water. Nevertheless, a solution of 5 M NaCl has a surface tension 8 mN/m above that of pure water (33,34). To further challenge the robustness of the constancy of surface tension, we spread myelin on 5 M NaCl and the equilibrium (and collapse) tension was again 27–28 mN/m. Correspondingly, the ESP and the collapse pressure are 52–53 mN/m. A speculation regarding the reason for the independency of the equilibrium surface tension on the initial surface tension is that the polar headgroup component of the tension may be quite relaxed at equilibrium in fluid monolayers (regardless on the subphase composition), but the hydrophobic component contribution (27 mN/m for hexadecane/air interface (29,35)) might not. In our view, the testing of the myelin system in solutions of aprotic solvents or high salt is a novel way of testing the hypothesis that the collapsed state of myelin monolayers is an equivalent condition to that in myelin bilayers (24).

Microscopy and SAXS

Because of the above arguments, when we compared the monolayer state to the one in bilayers we used relatively high monolayer surface pressure data, i.e., ~3–10 mN/m

below the collapse pressure. Observation of collapsed films is hard to interpret. Patterns potentially arising due to stacked multilayer (bi-, or trilayer) collapsed structures with planes of different surface patterns are difficult to differentiate from laterally segregated phase domains with the methodologies employed (24).

Water

The myelin monolayer on water shows homogeneity at high surface pressure, similar to our isolated myelin vesicles, showing a single spacing (155 Å) consistent with the 150–160 Å found in nerve CNS myelin in physiological conditions (1,13), and the 150 Å found in water as well in isolated CNS myelin in water (148–151 Å) (26). This value is roughly twice the value found for reconstituted lipid/protein bilayers and is due to the double bilayer asymmetric cell unit of myelin, which, in turn, is due to the bilayer asymmetry. The observation of the first-order Bragg peak with a relative intensity positioned similar to that in native myelin (1) suggest that the asymmetry of the membrane structure is well preserved, even to a larger extent than previously published for isolated myelin (14) prepared by the method of Norton and Poduslo (36); in fact, the first-order peak was absent for isolated myelins (13). To our knowledge, this is the first report showing preservation of first-order peak for isolated CNS myelin. In this regard, we employed an improved isolation method, a refinement of the original method of Norton and Poduslo, which has been shown to produce myelin of the highest purity (see Haley et al. (19)).

Adding solutes

The replacement of water by glycerol or glucose in water or in Ringer-based solutions does not have major effects on monolayers or on isolated myelin vesicles. This coincides with observations carried out on nerve myelin in Ringer's solutions after addition of those solutes (1). The addition of DMSO and DMF in distilled water changes the compression isotherm according to the lower surface tension of the subphases, but the films still get homogeneous before collapse, as in the case of water. Again, there is coincidence in the behavior of isolated myelin, which shows a single phase. No data for nerve myelin in these conditions are available in the literature. On the other hand, the introduction of NaCl in the physiological range (NaCl-water mixtures and Ringer solution) induces phase separation in monolayers as well as in myelin vesicles. This was also observed in nerve myelin, but at higher salt concentrations (3). The two-phase regime consists of a nearly normal period plus a thicker or expanded period phase. A thicker phase has been described for CNS myelin under certain conditions (26). Purified myelin lipid monolayers show a low-pressure critical mixing point (10). These critical points have been detected for other membrane systems (37,38). The criticality of mixing in whole myelin monolayers cannot be probed nor discarded from either Fig. 2 or 4. The mixing point is not affected by salt content in myelin lipid monolayers; nevertheless, when MBP is added, the ionic strength further causes an increase of the pressure for mixing, indicating a stabilization of the heterogeneous state (39) along the same trend than in this work.

The addition of Ca^{2+}, DMSO, or DMF to Ringer solutions leads to phase separation as also found in monolayers. In SAXS, we observed the appearance of a new overcompacted phase. This compaction agrees with the behavior observed in nerve myelin under Ca^{2+} (27) as well as after DMSO and DMF exposure (1,40) or in hypertonic (0.6–5 M NaCl) conditions (3); in fact, we ascertained that myelin vesicles show the same behavior in NaCl 4 M. Thus, the response of monolayer phase coexistence, isolated myelin vesicles, and nerve myelin to DMSO, DMF, and Ca^{2+} appears to be generally similar, even on semiquantitative terms, when bilayer spacings are compared. Moreover, the addition of Ca^{2+} 33 mM to pure water also leads to phase separation. An early explanation suggested that Ca^{2+}-induced domain segregation in nerve myelin multilayers was coupled to a closer apposition among adjacent bilayers with subsequent exclusion of proteins into laterally segregated domains (27). In the monolayer system, analogous protein-enriched domain segregation is equally induced by such subphase conditions, even if interaction with another surface is absent; thus, such contacts appear not to be necessary for phase separation. This is in agreement with previous observations in nerve myelin (3). The main divergence in the behavior of the three systems is that physiological salt concentration induces heterogeneity in myelin monolayers and myelin vesicles, but nerve myelin is homogeneous under those circumstances; this suggests the involvement of some other regulatory factor so far unknown. Most probably, physiological conditions set the membrane at the border of transitions (41) or at a critical state that turns them very sensitive to slight environmental modulation (42).

Environmental conditions including the presence of solutes and molecular packing, determine rather large differences in myelin lateral heterogeneity, which can result in a homogeneous or heterogeneous monolayer. This could be related to discrepancies found regarding isolated myelin raft composition using different detergents (43). Available data show that the correspondence of the structural phase behavior of myelin monolayers, myelin vesicles, and optic nerve myelin is remarkable (Table 2).

WAXS data

Normally, WAXS data from myelin systems at $T > 0°C$ do not show any Bragg peak from alkane chains but rather a smooth scattering over 4.3–4.8 Å ranges, coming from disordered acyl chains. This is the case for whole myelin as well as for its purified lipids. There is a noticeable

TABLE 2 Number of structural phases in different aqueous conditions for myelin monolayers at the air/aqueous interface (*first column*), isolated myelin membranes (*second column*), and CNS nerve myelin (*third column*, from (3))

Subphase-bulk media	Monolayer	Isolated myelin	CNS myelin
Water	1	1	1
Water glycerol 20%	1	1	1
Water sucrose 20%	1	1	NA
Water DMSO 20%	1	1	NA
Water DMF 20%	1	1	NA
Water NaCl 100 mM	2	2	NA
Water $CaCl_2$ 20–33 mM	2	2	NA
Ringer's	2	2	1
Ringer's $CaCl_2$ 20–33 mM	2	2	2
Ringer's glycerol 20%	2	2	1
Ringer's sucrose 20%	2	2	1
Ringer's DMSO 20%	2	2	2
Ringer's DMF 20%	2	2	2
TRIS $CaCl_2$ 20%	2	2	NA

NA, not available.

exception (44), and as far as we know, this is the only WAXS peaks reported for purified myelin lipids, suggesting a gel-liquid crystalline phase coexistence up to 60°C. Other work shows ordered alkane periodicity for whole nerve myelin, but this appears on cooling after freezing of residual water at ~−10°C (45). Here we report a clear Bragg peak but only for lyophilized myelin. The suspension of myelin in aqueous media leads to peak broadening typical of disordered acyl chains, as described in most of the myelin literature (46). We have previously shown liquid-liquid phase coexistence for purified myelin lipid monolayers only at very low surface pressure (i.e., at <3 mN/m); at higher surface pressure, only a single liquid phase is observed (10). In any case, only fluid phases are observed. The WAXS data in this article shows liquid-like acyl chain order. Therefore, if there is phase coexistence, it would be restricted to liquid-liquid immiscibility, in analogy to what is found in monolayers.

The basis for the monolayer-multilayer correspondence in phase separation

In a first consideration, it is immediately apparent that direct correlation of the phase behavior for myelin multilayers and monolayers encounters serious difficulties because the asymmetry of the native and isolated membrane is completely lost in the monolayer at the air/water interface, inasmuch as all polar moieties face the aqueous medium on the same side. In addition, transmembrane proteins (mainly Folch's proteolipid) are forced to adopt a different organization due to the stringent conditions imposed by the energetics and mechanical tensions of such interface. Nevertheless, there are some peculiarities in myelin that should be taken into account to rationalize the similarities found in the behavior of myelin monolayers and membranes.

The asymmetric composition of myelin is only partial

Cholesterol, the main lipid of myelin (mole fraction 0.4), and a major determinant of liquid-liquid immiscibility in biomembranes, is the more symmetrically distributed lipid, with a relation 2:1 between the cytoplasmic and extracellular hemihalves of the membrane.

Coupled behavior of the inner and outer myelin monolayer in vivo

The phase separation on myelin compaction affects both hemihalves of the membrane simultaneously. Furthermore, the compacted phase of myelin is in register over several bilayers; the same is true for the noncompacted normal period phase of myelin, bringing the epitaxial coupling to a higher hierarchical level. In fact, this allows diffraction to occur in the phase-separated system (3), even with the isolated membrane. All this indicates that the behavior of both hemihalves is similar, despite the compositional asymmetry of some components.

Cholesterol (and its enriched LO phases) does not interact favorably with lateral protein interfaces

Regardless of whether cholesterol is included in a bilayer or in a monolayer, or the protein is in a native conformation, cholesterol does not interact favorably with protein lateral interfaces (47). The integral Folch's proteolipid, the major CNS myelin protein, is phase-excluded from monolayers of total myelin lipids (10). MBP, the second major CNS myelin protein (a more peripheral protein), does not interact with the cholesterol-enriched phase and partitions into the LE phase (12).

Generally, the analogies between mono- and bilayers in the field of biomembranes were restricted to discussions of systems of pure lipids (and its simple mixtures) or containing lipid-peripheral proteins (30), but systems with integral membrane proteins are seldom studied with the exception of pulmonary surfactant (48). Our work shows that some consistent analogy can be extended to more-complex systems of membrane components containing integral proteins. In this regard, the myelin membrane represents a relatively unique bilayer system to compare because of its well-known particular architecture, capacity for formation of myelin vesicles amenable to use in diffraction techniques, and by the property of forming stable monolayers in which the surface composition and organization can be partially controlled (6).

CONCLUSIONS

Monolayer studies have provided new insights on the surface structural behavior formed by whole myelin and some of its isolated components. In previous work, we reported changes of domain morphology under compression of a myelin monolayer on a subphase containing 20 mM

Ca^{2+}. Now we found that deeper changes occur on compression as a function of the water milieu beneath the monolayer, not only modifying domain morphology, but also the very stability of the domains under compression. Myelin domain stability, distribution, and phase merging in monolayers are very sensitive to slight variations of the surface pressure (molecular packing) and the composition of the interface formed with some purified lipid and protein myelin components (6,10,12). These conditions are either not easy or impossible to vary at will in vivo or in myelin vesicles. Moreover, the presence and coexistence of laterally segregated surface phases in monolayers show a generally good correspondence with the phase behavior of isolated myelin vesicles and with several structural features of nerve myelin.

SUPPORTING MATERIAL

One movie is available at http://www.biophysj.org/biophysj/supplemental/S0006-3495(10)00796-4.

We thank HASYLAB-Deutsches Elektronen Synchrotron (DESY), Hamburg, Germany (beamline A2 at DORIS) and Laboratório Nacional de Luz Síncrotron, Campinas, Brazil (beamline SAXS2) for measurement times.

This work was supported by Consejo Nacional de Investigaciones Científicas y Técnicas (CONICET), Fundación Antorchas, Fondo para la Investigación Científica y Tecnológica (FONCyT), and Secretaría de Ciencia y Tecnológia, University of Cordoba (SECyT-UNC). R.G.O. and B.M. are career investigators of CONICET (Argentina). R.G.O. thanks the Alexander von Humboldt Foundation for a postdoctoral research fellowship.

REFERENCES

1. Kirschner, D. A., A. L. Ganser, and D. L. Caspar. 1984. Diffraction studies of molecular organization and membrane interactions in myelin. *In* Myelin. P. Morell, editor. Plenum Press, New York.
2. Inouye, H., and D. A. Kirschner. 1988. Membrane interactions in nerve myelin. I. Determination of surface charge from effects of pH and ionic strength on period. *Biophys. J.* 53:235–245.
3. Hollingshead, C. J., D. L. Caspar, …, D. A. Kirschner. 1981. Compaction and particle segregation in myelin membrane arrays. *J. Cell Biol.* 89:631–644.
4. Finean, J. B., R. Coleman, …, A. R. Limbrick. 1966. Low-angle x-ray diffraction and electron-microscope studies of isolated cell membranes. *J. Cell Sci.* 1:287–296.
5. Joy, R. T., and J. B. Finean. 1963. A comparison of the effects of freezing and of treatment with hypertonic solutions on the structure of nerve myelin. *J. Ultrastruct. Res.* 8:264–282.
6. Rosetti, C. M., B. Maggio, and R. G. Oliveira. 2008. The self-organization of lipids and proteins of myelin at the membrane interface. Molecular factors underlying the microheterogeneity of domain segregation. *Biochim. Biophys. Acta.* 1778:1665–1675.
7. Oliveira, R. G., R. O. Calderón, and B. Maggio. 1998. Surface behavior of myelin monolayers. *Biochim. Biophys. Acta.* 1370:127–137.
8. Oliveira, R. G., and B. Maggio. 2000. Epifluorescence microscopy of surface domain microheterogeneity in myelin monolayers at the air-water interface. *Neurochem. Res.* 25:77–86.
9. Oliveira, R. G., and B. Maggio. 2002. Compositional domain immiscibility in whole myelin monolayers at the air-water interface and Langmuir-Blodgett films. *Biochim. Biophys. Acta.* 1561:238–250.
10. Rosetti, C. M., R. G. Oliveira, and B. Maggio. 2005. The Folch-Lees proteolipid induces phase coexistence and transverse reorganization of lateral domains in myelin monolayers. *Biochim. Biophys. Acta.* 1668:75–86.
11. Oliveira, R. G., M. Tanaka, and B. Maggio. 2005. Many length scales surface fractality in monomolecular films of whole myelin lipids and proteins. *J. Struct. Biol.* 149:158–169.
12. Rosetti, C. M., and B. Maggio. 2007. Protein-induced surface structuring in myelin membrane monolayers. *Biophys. J.* 93:4254–4267.
13. Sedzik, J., and A. E. Blaurock. 1995. Myelin vesicles: what we know and what we do not know. *J. Neurosci. Res.* 41:145–152.
14. Inouye, H., J. Karthigasan, and D. A. Kirschner. 1989. Membrane structure in isolated and intact myelins. *Biophys. J.* 56:129–137.
15. MacDonald, R. C., and S. A. Simon. 1987. Lipid monolayer states and their relationships to bilayers. *Proc. Natl. Acad. Sci. USA.* 84: 4089–4093.
16. Gershfeld, N. L. 1989. The critical unilamellar lipid state: a perspective for membrane bilayer assembly. *Biochim. Biophys. Acta.* 988:335–350.
17. Nag, K., J. S. Pao, …, L. A. Bagatolli. 2002. Segregation of saturated chain lipids in pulmonary surfactant films and bilayers. *Biophys. J.* 82:2041–2051.
18. Dietrich, C., L. A. Bagatolli, …, E. Gratton. 2001. Lipid rafts reconstituted in model membranes. *Biophys. J.* 80:1417–1428.
19. Haley, J. E., F. G. Samuels, and R. W. Ledeen. 1981. Study of myelin purity in relation to axonal contaminants. *Cell. Mol. Neurobiol.* 1: 175–187.
20. Bianco, I. D., G. D. Fidelio, and B. Maggio. 1988. Effect of glycerol on the molecular properties of cerebrosides, sulphatides and gangliosides in monolayers. *Biochem. J.* 251:613–616.
21. Hönig, D., and D. Möbius. 1991. Direct visualization of monolayers at the air-water interface by Brewster angle microscopy. *J. Phys. Chem.* 95:4590–4592.
22. Hénon, S., and J. Meunier. 1991. Microscope at the Brewster angle: direct observation of first-order phase transitions in monolayers. *Rev. Sci. Instrum.* 62:936–939.
23. Ginsberg, L., D. L. Gilbert, and N. L. Gershfeld. 1991. Membrane bilayer assembly in neural tissue of rat and squid as a critical phenomenon: influence of temperature and membrane proteins. *J. Membr. Biol.* 119:65–73.
24. Oliveira, R. G., and B. Maggio. 2003. Surface behavior, microheterogeneity and adsorption equilibrium of myelin at the air-water interface. *Chem. Phys. Lipids.* 122:171–176.
25. Janiak, M. J., D. M. Small, and G. G. Shipley. 1976. Nature of the thermal pretransition of synthetic phospholipids: dimyristoyl- and dipalmitoyllecithin. *Biochemistry.* 15:4575–4580.
26. Karthigasan, J., and D. A. Kirschner. 1988. Membrane interactions are altered in myelin isolated from central and peripheral nervous system tissues. *J. Neurochem.* 51:228–236.
27. Melchior, V., C. J. Hollingshead, and D. L. Caspar. 1979. Divalent cations cooperatively stabilize close membrane contacts in myelin. *Biochim. Biophys. Acta.* 554:204–226.
28. Marsh, D. 1996. Lateral pressure in membranes. *Biochim. Biophys. Acta.* 1286:183–223.
29. Feng, S. 1999. Interpretation of mechanochemical properties of lipid bilayer vesicles from equation of state or pressure-area measurements of the monolayer at the air-water interface or oil-water interface. *Langmuir.* 15:998–1010.
30. Brockman, H. 1999. Lipid monolayers: why use half a membrane to characterize protein-membrane interactions? *Curr. Opin. Struct. Biol.* 9:438–443.
31. Feng, S. 2006. Reply to comment on interpretation of mechanochemical properties of lipid bilayer vesicles from the equation of state or pressure-area measurement of the monolayer at the air-water or oil-water interface. *Langmuir.* 22:2920–2922.

32. Marsh, D. 2006. Comment on interpretation of mechanochemical properties of lipid bilayer vesicles from the equation of state or pressure-area measurement of the monolayer at the air-water or oil-water interface. *Langmuir.* 22:2916–2919, discussion 2920–2922.

33. Adamson, A. W. 1967. Physical Chemistry of Surfaces. Interscience Publishers, John Wiley & Sons, New York.

34. Collins, K. D., and M. W. Washabaugh. 1985. The Hofmeister effect and the behavior of water at interfaces. *Q. Rev. Biophys.* 18:323–422.

35. Lu, W., C. M. Knobler, …, M. Dennin. 2002. Folding Langmuir monolayers. *Phys. Rev. Lett.* 89:146107.

36. Norton, W. T., and S. E. Poduslo. 1973. Myelination in rat brain: method of myelin isolation. *J. Neurochem.* 21:749–757.

37. Keller, S. L., W. H. Pitcher, III, …, H. M. McConnell. 1998. Red blood cell lipids form immiscible liquids. *Phys. Rev. Lett.* 81:5019–5022.

38. Veatch, S. L., P. Cicuta, …, B. Baird. 2008. Critical fluctuations in plasma membrane vesicles. *ACS Chem. Biol.* 3:287–293.

39. Rosetti, C. M., B. Maggio, and N. Wilke. 2010. Micron-scale phase segregation in lipid monolayers induced by myelin basic protein in the presence of a cholesterol analog. *Biochim. Biophys. Acta.* 1798:498–505.

40. da Silva, P. P., and R. G. Miller. 1975. Membrane particles on fracture faces of frozen myelin. *Proc. Natl. Acad. Sci. USA.* 72:4046–4050.

41. Lingwood, D., J. Ries, …, K. Simons. 2008. Plasma membranes are poised for activation of raft phase coalescence at physiological temperature. *Proc. Natl. Acad. Sci. USA.* 105:10005–10010.

42. Jin, A. J., M. Edidin, …, N. L. Gershfeld. 1999. A singular state of membrane lipids at cell growth temperatures. *Biochemistry.* 38:13275–13278.

43. Taylor, C. M., T. Coetzee, and S. E. Pfeiffer. 2002. Detergent-insoluble glycosphingolipid/cholesterol microdomains of the myelin membrane. *J. Neurochem.* 81:993–1004.

44. Chia, L. S., J. E. Thompson, and M. A. Moscarello. 1984. Alteration of lipid-phase behavior in multiple sclerosis myelin revealed by wide-angle x-ray diffraction. *Proc. Natl. Acad. Sci. USA.* 81:1871–1874.

45. Finean, J. B., and A. L. Hutchinson. 1988. X-ray diffraction studies of lipid phase transitions in cholesterol-rich membranes at sub-zero temperatures. *Chem. Phys. Lipids.* 46:63–71.

46. Franks, N. P., V. Melchior, …, D. L. Caspar. 1982. Structure of myelin lipid bilayers. Changes during maturation. *J. Mol. Biol.* 155:133–153.

47. Epand, R. M. 2004. Do proteins facilitate the formation of cholesterol-rich domains? *Biochim. Biophys. Acta.* 1666:227–238.

48. Pérez-Gil, J. 2008. Structure of pulmonary surfactant membranes and films: the role of proteins and lipid-protein interactions. *Biochim. Biophys. Acta.* 1778:1676–1695.